PERFORMANCE OF JOINT CONNECTIONS BETWEEN DECKED PRESTRESSED CONCRETE BRIDGE GIRDERS

Huijun Dong, CEE Department, Michigan Technological University, MI
Yue Li, Ph.D., CEE Department, Michigan Technological University, MI
Theresa M. Ahlborn, Ph.D, PE, CEE Department, Michigan Technological University, MI

ABSTRACT

Decked prestressed concrete girder bridges systems are used in the United States as an effective solution for rapid construction. The performance of longitudinal joint connections between two adjacent girders, key components of such systems, requires thorough investigation to better understand joint behavior. In this paper, the influence of joint connection rigidity is examined through two extreme cases in the whole bridge models–fully fixed or hinged. Three typical in-use bridge joint configurations are investigated in detail. Finite element joint models are analyzed using the resulting force obtained from a full bridge model. Effects of strength of the grout material, different load directions and three joint configurations (A, B, and C) on joint connection performance are investigated. It is found that the Joint Model A has the best performance and no cracking is observed in the joint zone, while severe stress concentrations and cracking occurred in Joint Models B and C. Higher strength grout material would not alleviate the situation. Effects of load configurations, diaphragm placement and deck post-tensioning are discussed.

Keywords: Connections; Decked girders; Finite element analysis; Grout material; Prestressed concrete girders; Rapid construction

INTRODUCTION

Prefabricated, prestressed concrete girder bridge systems have had limited regional use in the United States for several decades even though the system leads to rapid construction, lower equipment cost and good structural durability. Decked girder systems further enhance these benefits. However, the joint connections between decked girders, an important component of this bridge system, have attracted researchers' attention in recent years. Issa et al.[1,2] surveyed the current state of precast, prestressed concrete bridge systems of individual states in the U. S., including the construction types, deck and panel dimensions, joint connecting system, and the materials used in connectors. A total of 36 full scale specimens with different grout materials were tested by Issa et al.[3], for direct tension, vertical shear and flexural capacity using different test setups. Corresponding modes of failure and shear capacity of joint connections were evaluated by Finite Element Analysis (FEA). Rapid setting grout was recommended in joint connections due to its ease of use and good performance. Issa et al.[4] used push-out tests to study the failure patterns of shear connectors between the bridge deck and the precast/prestressed concrete girders. FEA analysis was compared with the testing results and the provisions in AASHTO LRFD[5]. Menkulasi and Roberts-Wollmann[6] carried out 36 push-off tests to investigate the behavior of horizontal shear connections. Two different grout materials, three haunch heights and several alternate connector configurations were considered. They concluded that Set 45 grout could provide a higher shear stresses comparing with latex modified grout; no significant effect on shear stresses were observed between tests with variable haunch heights; different horizontal shear connectors could be used in such bridge system. Shah et al.[7] reported the field testing results of four concrete decked bridge girders and discussed the load-response behavior, load capacity and failure modes. Four moment connections and six bridge models in total were tested. Results showed that the location of the wheel load affects the load-carrying capacity of the various connections.

Most of previous research focused on the study of individual force capacity of the joint connections, while little study was carried out on the longitudinal joint behavior under the combined loads. Also, the effects of transverse post-tensioning and intermediate diaphragms need to be investigated. This study is to demonstrate how the joint connections behave under combined loads using the finite element method. In this paper, whole bridge models are briefly presented to explain how to extract the loads applied to joint models. Joint models are then analyzed in detail to get an indication of longitudinal joint behavior, considering joint configurations, transverse post-tensioning and diaphragm placement.

FINITE ELEMENT ANALYSIS OF BRIDGE

A typical decked prestressed concrete bridge superstructure, as shown in Figure 1, constitutes the basis of this study. A total of ten 100-ft pretopped I-girder bridge cases with different diaphragm locations, post-tensioning levels, and analyzing conditions are modeled in GTStrudl (Version 28). Four load cases (M1, M2, V1, and V2) are analyzed for each whole bridge model, load cases "M1" and "M2" represent one and two HL-93

trucks, respectively, applied in combination with the lane load and located so as to induce the absolute maximum moment in the bridge girders. Similarly, load cases V1 and V2 represent one or two trucks located to induce maximum shear. Based on the Section 3.6.2.1 of the AASHTO LRFD[5], an impact factor 1.33 is considered for the bridge analysis.

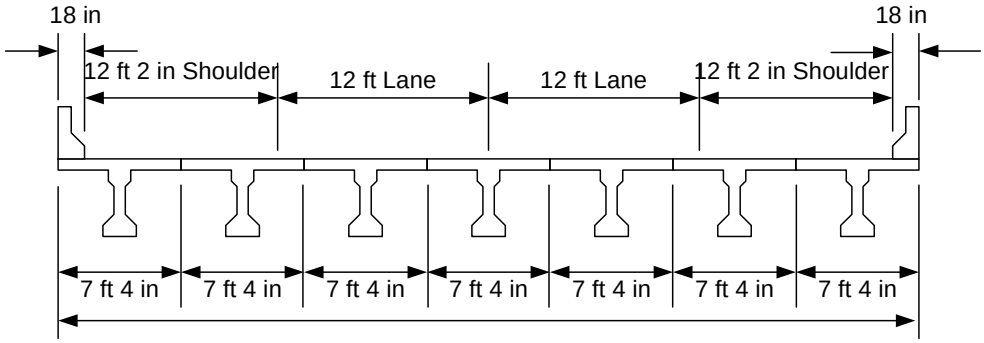

Figure 1 Bridge Cross-Section

Seven decked girders using the AASHTO Type III I-beam constitute the whole bridge model. This study focuses on the behavior of horizontal connections between adjacent girders. To simplify the models and accelerate the analysis, the joint connections are represented by a series of joint ties along the girders. In the ten whole bridge models, fully fixed ties are used in five models, and hinged ties are used in the others. The detailed information of all the models is listed in Table 1.

Table 1 Full Bridge Model Summary

Model	Fixed Joint	Hinged Joint	Diaphragms*			Post-Tensioning **	
			0	1	2	Yes	No
a	X		X				X
b		X	X				X
c	X			X			X
d		X		X			X
e	X				X		X
f		X			X		X
g	X		X			X	
h		X	X			X	
i	X			X		X	
j		X		X		X	

* Single diaphragm placed at midspan; two diaphragms placed at third points
** Post-tensioning through mid level of deck at 250 psi

From the results of whole bridge model analysis, four forces are observed to primarily influence the performance of the longitudinal joint connections. These forces are transverse normal forces, transverse bending moment, vertical shear and horizontal shear. The maximum horizontal shear occurred at the end of the bridge, while the maximums of other three occur at the location of the truck wheels. Detailed information about whole bridge models can be found in the final research report[8] (to be submitted).

In reality, the longitudinal connections between adjacent decked girders are neither fixed nor hinged but behave somewhere between. The full bridge model analysis gives upper and lower bounds for longitudinal joint forces under design loads. To further study joint behavior, the model with highest combination from applied loads, Model (i) is selected. This model includes fixed joint ties, midspan intermediate diaphragm and post-tensioning.

LOADS FOR JOINT MODELS

The loads applied for joint models result from of the full bridge analysis of Model (i), where design load cases 'M2' and 'V2' govern. Six longitudinal joints are reviewed, with highest impact along the joint inline with wheel loads nearest mid-width of the bridge fourth joint from left in Figure 1. The highest values of the four resulting joint stresses occur at different locations along the joint length. Horizontal shear is largest at 1.5 ft and other stresses reach their peaks at 38 ft, as illustrated in Figure 2 for a typical case.

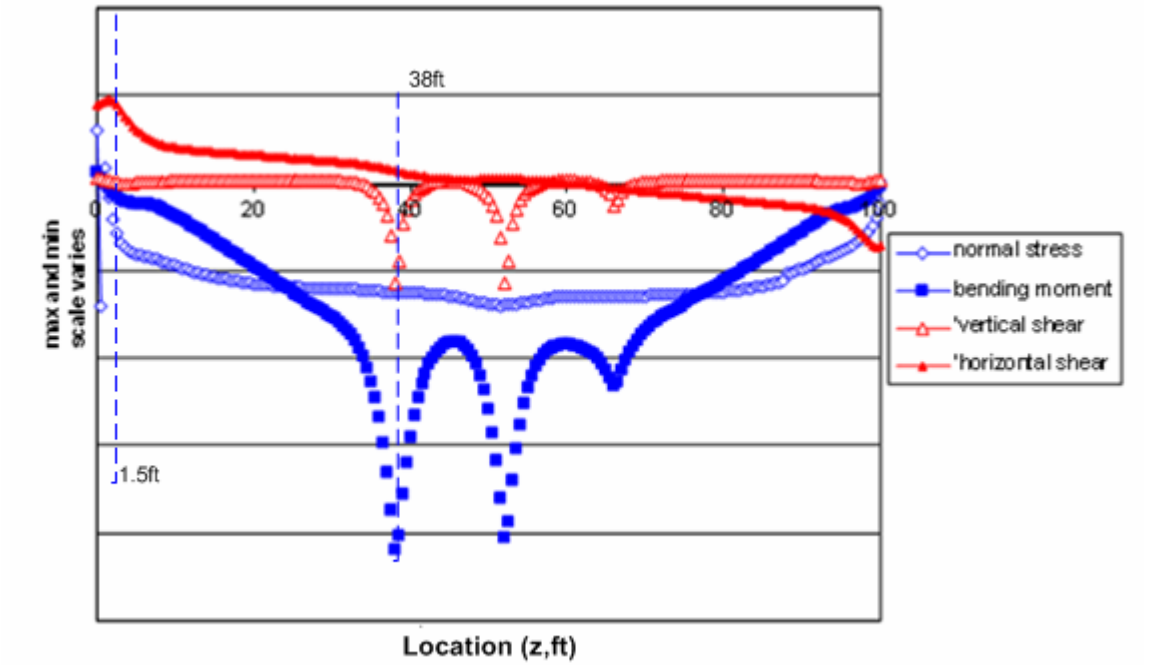

Figure 2 Internal Forces at Joint along the Span of Bridge

JOINT MODELS

JOINT CONFIGURATION IDENTIFICATION

Several joint connection details are collected from a number of sources to demonstrate the variety of shear key details used in precast full depth concrete bridge decks in the United States. For the purpose of this paper, three joints - A, B and C (Figure 3) - are selected for further study.

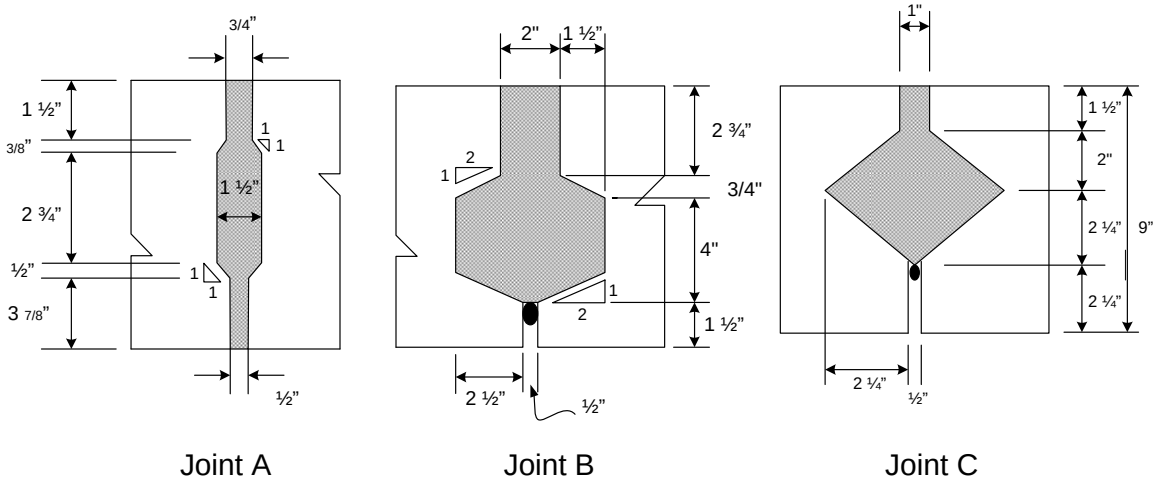

Figure 3 Three Joint Configurations

MODELING

A 3-D cantilever finite element model (Figure 4) with a fixed right surface is used to model the detailed joint connection. The study focuses on the behavior of joint connections, therefore, the edge of the model is far enough from the joint zone so boundary conditions will not influence the behavior of the joint. The joint connection model is 48 inches long by 9 inches in height (the thickness of the bridge deck), with a thickness of 12 inches along the joint length.

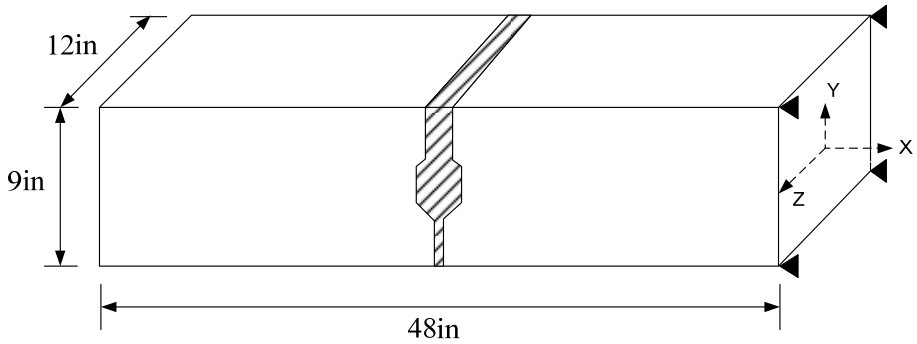

Figure 4 Finite Element Model for Joint Connection

A total of nine finite element joint models are investigated using the applied loading from the full bridge Model (i). Three different joint connection configurations (A, B and C) are used in a parametric study to determine the sensitivity of joint behavior with three different grout strengths. ABAQUS is used to model the joint connections, with two types of elements (4-node tetrahedron element and 8-node brick element). Finer mesh is applied around the joint core area and surface to surface constraints are added to assure compatibility between the joint zone and slab. A detailed mesh for Joint Model A is shown in Figure 5. The foam backer rod in the B and C models is not included.

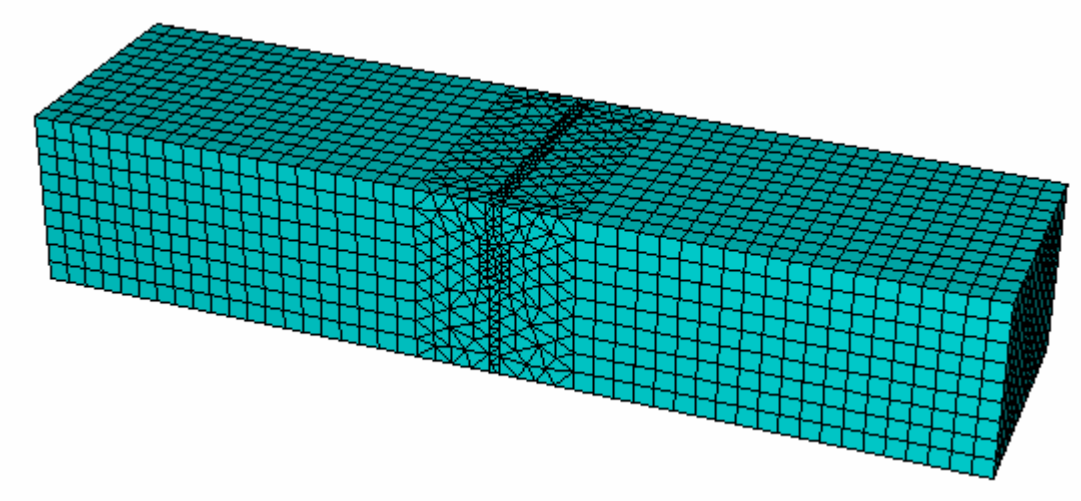

Figure 5 Finite Element Model of Joint A

MATERIALS

Two types of materials are defined in the joint model shown in Figure 4. The bridge deck and the joint connections are defined as 'concrete' and 'grout', respectively. For FEA models,the concrete strength is assumed to be 7 ksi typical of a decked prestressed girder, while three different grout strengths are considered to examine the effect of grout material strength on joint connection performance. The tension (cracking) strengths are calculated based on $0.19(f_c')^{0.5}$ (f_c' in ksi). The assumed material properties used in modeling are summarized in Table 2.

Table 2 Material Properties for Detailed Joint Models

	Concrete	Grout (0.5 f_c')	Grout (1 f_c')	Grout(1.5f_c')
Compressive strength f_c' (ksi)	7	3.5	7	10.5
Tensile strength f_t (ksi)	0.503	0.355	0.503	0.615
Young's Modulus(ksi)	5070	3590	5070	6210
Shear Modulus(ksi)	2110	1500	2110	2590
Poisson's Ratio	0.2	0.2	0.2	0.2
Material density(lbs/ft^3)	8.68E-5	8.68E-5	8.68E-5	8.68E-5

Note: 0.5, 1 and 1.5 refer to the ratio of the strength of grout to that of concrete.

LOADING

To study longitudinal joint performance, four Joint Load Cases (JLC) are applied to the joint models. For load case 'M2', two locations (1.5 and 38 ft) are defined as JLC1 and JLC2, respectively. JLC3 (M2max) and JLC4 (V2max) are governed by the maximum internal forces under load cases 'M2' and 'V2' instead of any specific location along the joint-line. The internal forces in the joint connection (normal stress, transverse bending moment, vertical shear stress and horizontal shear stress) from JLC 1-4, are extracted from the full bridge analysis and applied to the detailed joint models.

Applying loads from the whole bridge to the detailed joint models is accomplished as follows. The normal stress is represented by the surface pressure of the elements on the left surface of the model, and the vertical shear is generated by nodal loads at the left edge, which is 24 inches from the joint center (Figure 6(a)). The transverse bending moment on the joint region is applied by two sources: the moment caused by the vertical shear loads and moment couples acting on the left surface of the model. Horizontal shear (Figure 6(b)) is generated by nodal forces, and another couple is added to eliminate the moment induced in the joint due to the applied horizontal shear load. The detailed loads are listed in Table 3.

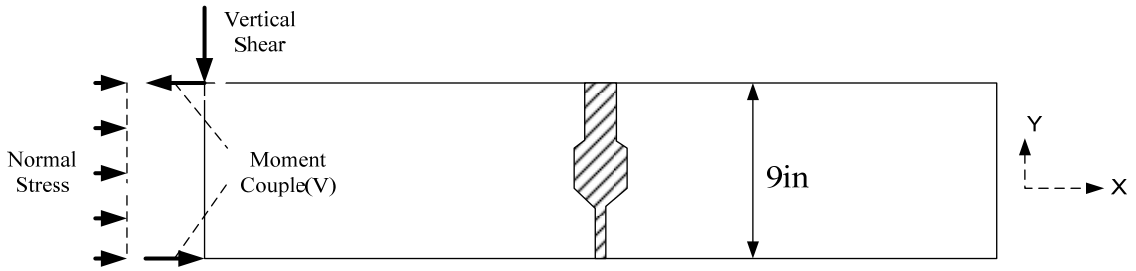

Figure 6 (a) Applied Normal Stress, Vertical Shear and Bending Moment on Joint Model

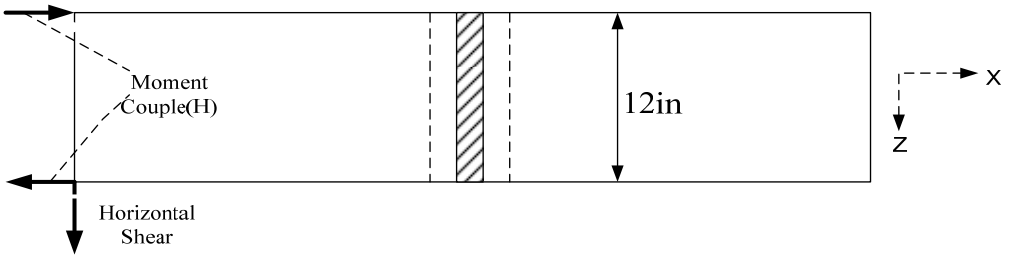

Figure 6 (b) Applied Horizontal Shear on Joint Model

Table 3 Applied Loads for Detailed Joint Connection

Joint Load Cases	Joint Model (Figure 2)	Compression (ksi)	Vertical Shear (kip)	Couple Force(V) (kip)	Horizontal Shear (kip)	Couple Force(H) (kip)
JLC1 1.5ft (M2)	A	-0.084	0.072	0.061	0.2897	0.5795
	B				0.8926	1.7851
	C				0.5065	1.0131
JLC2 38ft (M2)	A	-0.251	2.157	2.762	0.0247	0.0494
	B				0.0761	0.1523
	C				0.0432	0.0864
JLC3 M2max	A	-0.251	2.178	2.702	0.2897	0.5795
	B				0.8926	1.7851
	C				0.5065	1.0131
JLC4 V2max	A	-0.267	2.203	1.266	0.2995	0.5990
	B				0.9227	1.8455
	C				0.5236	1.0473

JOINT BEHAVIOR RESULTS

Nine joint models are evaluated (Three joint connection configurations with three grout strengths each). Joint Model A with different grout materials is analyzed under the four Joint Load Cases (total 12 cases). Based on the results of Joint A, only 7 cases are considered for Joints B and C (see in Table 4). Sensitivity analysis is conducted to determine the effect of load directions, grout strength, and joint connection configurations on the maximum principle stress distribution around the joint.

Table 4 Maximum Principle Stress in the Joint Region (ksi)

Model	Load case	$f_g^{'} = 0.5 f_c^{'}$	$f_g^{'} = 1 f_c^{'}$	$f_g^{'} = 1.5 f_c^{'}$
		Cracking stress 0.355ksi	Cracking stress 0.503ksi	Cracking stress 0.615ksi
A	JLC1	0.0038	0.0044	0.0086
	JLC 2	0.2688	0.2699	0.2709
	JLC 3	0.2824	0.2833	0.2841
	JLC 4	0.2024	0.2028	0.2035
B	JLC 1	-----	-----	-----
	JLC 2	0.5825	0.6101	0.6224
	JLC 3	0.5896	0.6165	0.6284
	JLC 4	-----	0.2433	-----
C	JLC 1	-----	-----	-----
	JLC 2	0.5610	0.6452	0.6911
	JLC 3	0.5463	0.6334	0.6812
	JLC 4	-----	0.2161	-----

* Shaded cells indicate stress above cracking limit

EFFECTS OF LOADING DIRECTION

The applied loads are shown in Figure 6(a) and 6(b) for Joint Model A (f_g' = f_c'). Analyses are conducted to compare the difference in stress distributions. The maximum principal stress in the joint is shown in Figure 7. The effect of reverse load directions needs to be considered because the joints are not symmetric along the depth of the deck. The directions of vertical shear and transverse bending moment in Figure 6(a) are reversed to represent the reverse loading conditions, and the maximum principal stress is demonstrated in Figure 8. The load case for both load directions is JLC2. From Figures 7 and 8, the maximum principle stresses under the two reverse load directions are almost symmetrical with a difference less than 10%, although the joint shapes are not symmetric. Similar results are observed in other joint configurations (B and C) and under other joint load cases (JLC1, 3 and 4). For instance, the maximum principal stress appeared at the bottom of the joint is 0.27ksi in Figure 7, while its counterpart at the top of the joint in Figure 8 is 0.29ksi. In the following analyses, only load directions shown in Figure 6 are considered.

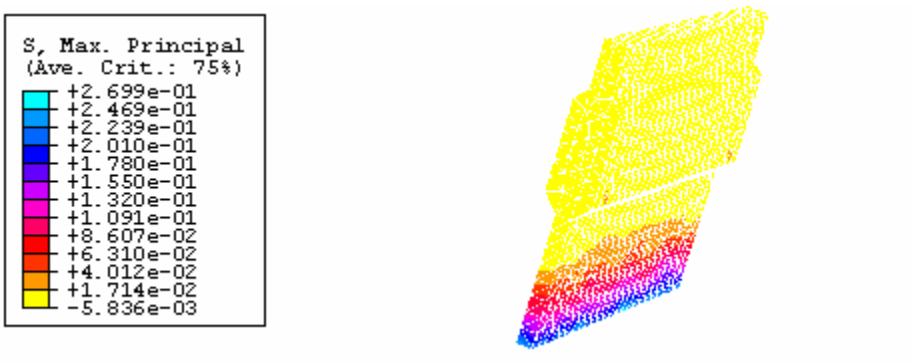

Figure 7 Maximum Principle Stress of Joint Model A (JLC2)

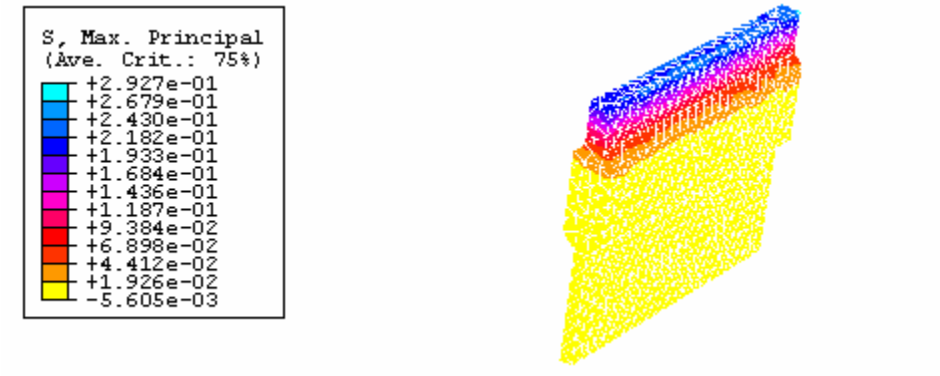

Figure 8 Maximum Principle Stress of Joint Model A (JLC2 with reversed loading)

EFFECTS OF GROUT MATERIALS

The effect of grout strength on the joint connection behavior is investigated by choosing the grout strength of 0.5, 1, and 1.5 times that of bridge deck concrete. Figures 9-11 show the maximum principle tension stress distributions under JLC2 (M2 38ft) for the Joint Model B.

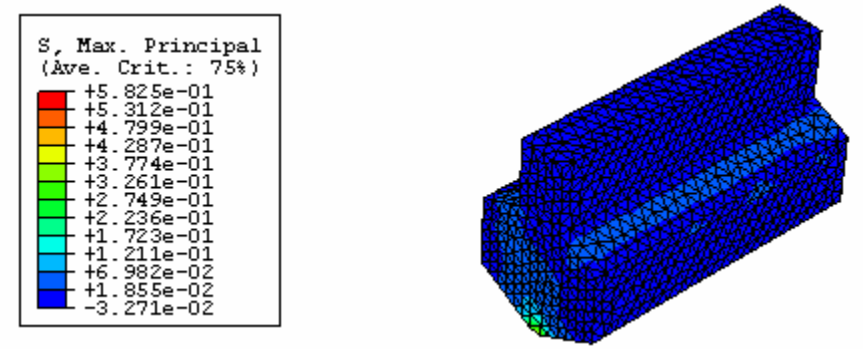

Figure 9 Maximum Principle Stress of Joint Model B (f_g' =0.5 f_c', JLC2)

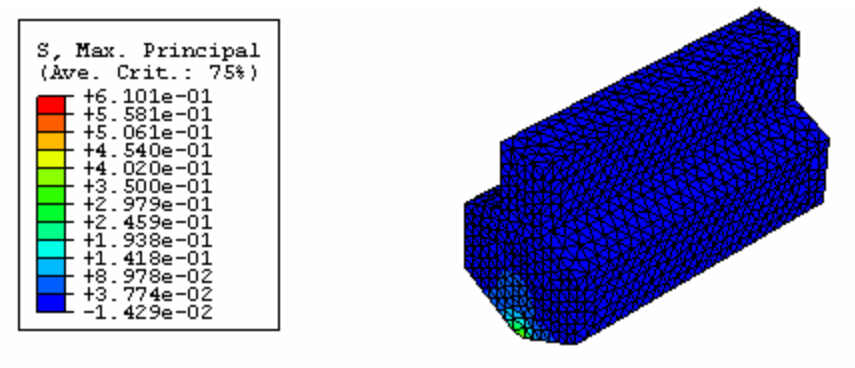

Figure 10 Maximum Principle Stress of Joint Model B (f_g' = f_c', JLC2)

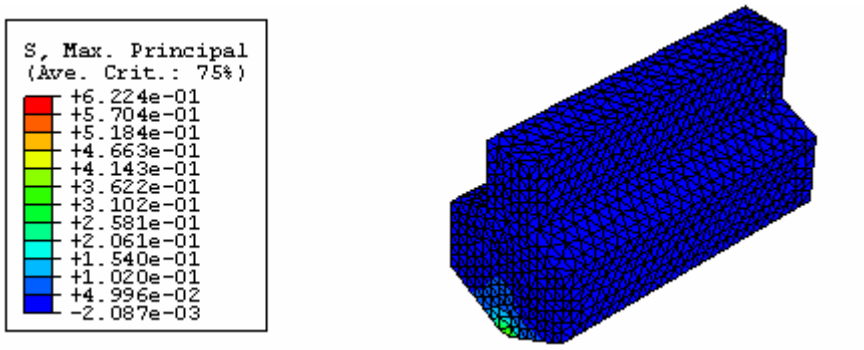

Figure 11 Maximum Principle Stress of Joint Model B (f_g' =1.5 f_c', JLC2)

By comparing stress distributions, Figure 9 through 11 show that with the increase of the grout material strength, the maximum principle stress at the joint zone does not vary greatly (see Table 4). However, the FEA shows the depth of cracking will be decreased with stronger grouts. Similar results are observed for joint connection models A and C. The only difference is that no cracking was observed in Joint Model A. The maximum principle tensile stresses of all analyzed load cases are summarized in Table 4.

EFFECTS OF JOINT CONFIGURATIONS

To consider the effect of joint configuration on joint behavior under design loading, only one grout strength (f_g' =0.5 f_c') can be isolated for joint comparison. JLC1 is previously found to be negligible. JLC2 and JLC3 (in Table 4) show the maximum principle stresses higher than cracking for the Joint Models B and C, which are not full depth (Figure 2). However, Joint Model A is not shown to crack, indicating that joint configuration has a significant impact on expected joint behavior. Figures 12 through 14 show the maximum principle stress under JLC2 for three joint connections.

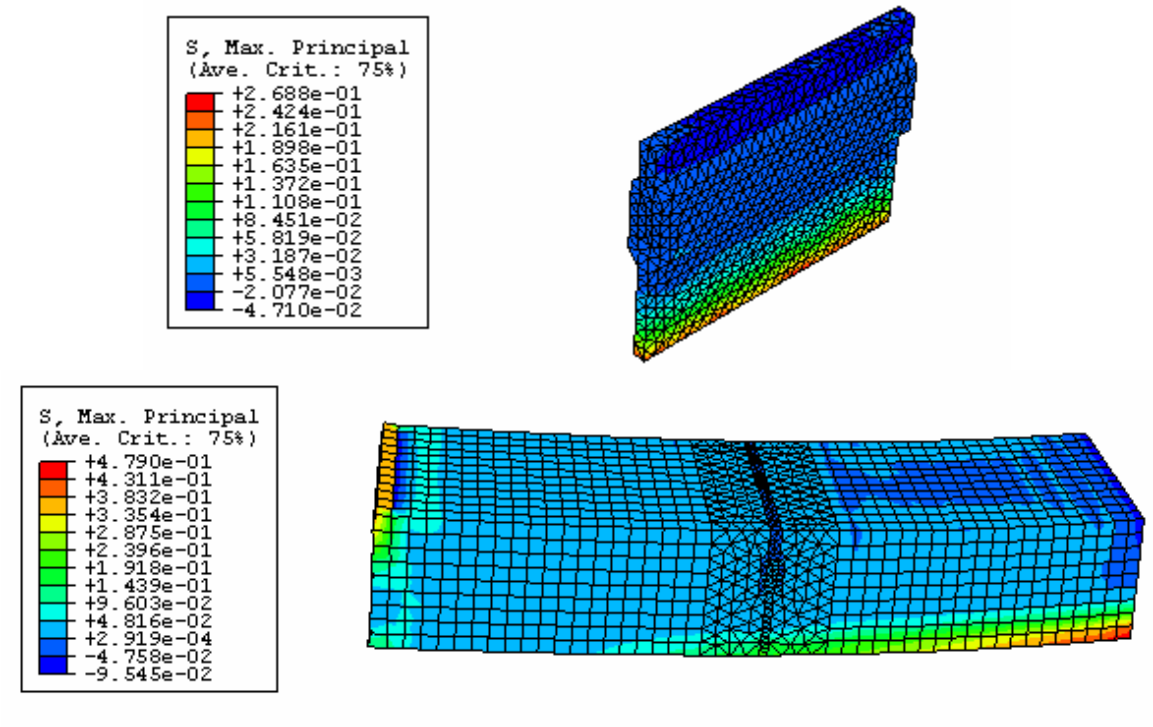

Figure 12 Maximum Principle Tension Stress of Joint Model A (JLC2)

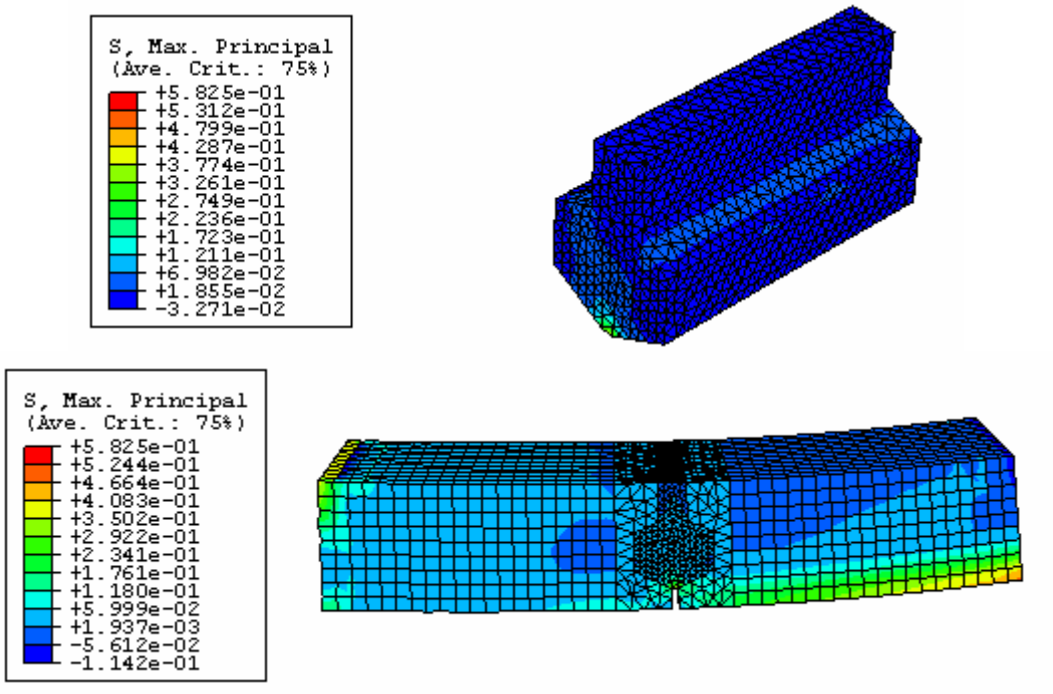

Figure 13 Maximum Principle Tension Stress of Joint Model B (JLC2)

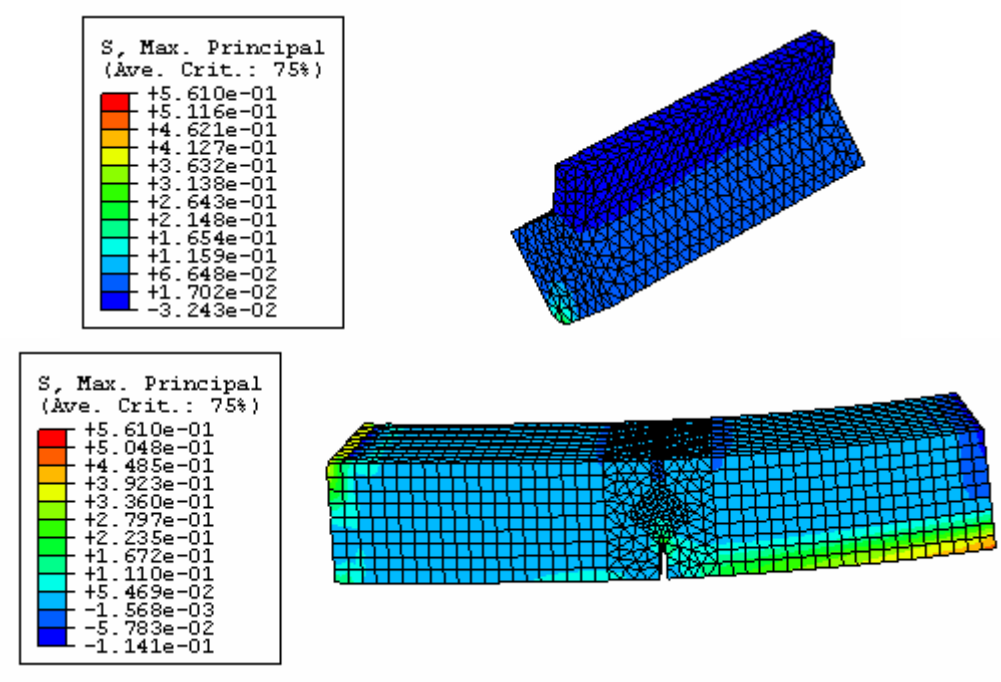

Figure 14 Maximum Principle Tension Stress of Joint Model C (JLC2)

CONCLUSIONS AND FUTURE WORK

The following conclusions can be made for stress distributions from various joint connection configurations:

- No grout cracking occurs in the Joint Model A, while the grout cracks in the Joint Models B and C, regardless of the strength of the grout material, indicating that joint configuration can significantly impact joint behavior. Full depth joints appear to behave better. Using grout material with a higher strength will decrease the depth of cracking.
- Compared with other loads, horizontal shear does not affect the joint behavior and could be neglected in future analysis.
- Stress concentrations are observed near the bottom openings of Joint Models B and C. The abrupt change in depth at the joint location causes these concentrations.
- In this study, only elastic behavior of the models with assumed material properties is considered. Further research on the joint connections with actual grout materials and nonlinear analysis method might be needed. Experimental verification is expected in a following project.

ACKNOWLEDGEMENTS

The authors gratefully acknowledge the sponsor of this funded research project, the Michigan Department of Transportation (MDOT), as well as project managers Roger Till and Steve Kahl, and members of the MDOT Research Advising Panel for guidance and suggestions throughout the course of this project.

REFERENCES

1. Issa M. A., Yousif A. A., Issa M. A., "Field Performance of Full Depth Precast Concrete Panels in Bridge Deck Reconstruction," *PCI Journal,* Vol. 40, No. 3, May-Jun 1995, pp. 82-107.

2. Issa M. A., Idriss A., and Kaspar I. I., "Full Depth Precast and Precast, Prestressed Concrete Bridge Deck Panels," *PCI Journal*, Vol. 40, No. 1, Jan-Feb 1995, pp. 59-80.

3. Issa M. A., Ribeiro do Valle C. L., and Abdalla H. A., "Performance of Transverse Joint Grout Materials in Full-Depth Precast Concrete Bridge Deck Systems," *PCI Journal,* Vol. 48, No. 4, Jul-Aug 2003, pp. 92-103.

4. Issa M. A., Salas J. S., and Shabila H. I., "Composite Behavior of Precast Concrete Full-Depth Panels and Prestressed Girders," *PCI Journal,* Vol. 51, No. 5, Sep-Oct 2006, pp. 132-145.

5. American Association of State Highway and Transportation Officials (AASHTO) AASHTO 3rd Edition LRFD Bridge Design Specifications (2006 interims).

6. Menkulasi F., and Roberts-Wollmann C. L., "Behavior of Horizontal Shear Connections for Full-Depth Precast Concrete Bridge Decks on Prestressed I-Girders," *PCI Journal*, V. 50, No. 3, May-June 2005, pp. 60-73.

7. Shah B. N., Lam C., and Sennah K. M., "Flange-to-Flange moment Connections for Precast Concrete Deck Bulb-Tee Bridge Girders," *PCI Journal,* Vol. 51, No. 6 Nov-Dec 2006, pp. 86-107.

8. Ahlborn, T. M., Li, Y., Dong, H., and Pipkorn, T. M. "Development of Rapid Construction Solutions Using Prefabricated Prestressed Concrete Systems-Phase I", Center for Structural Durability (CSD – 2007 – 10), Michigan Tech Transportation Institute, MDOT Report, MI, 2007.